



HAL
open science

Ultrashort Peptide Hydrogels Display Antimicrobial Activity and Enhance Angiogenic Growth Factor Release by Dental Pulp Stem/Stromal Cells

Marina E Afami, Ikhlas El Karim, Imad About, Sophie M Coulter, Garry Lavery, Fionnuala T Lundy

► **To cite this version:**

Marina E Afami, Ikhlas El Karim, Imad About, Sophie M Coulter, Garry Lavery, et al.. Ultrashort Peptide Hydrogels Display Antimicrobial Activity and Enhance Angiogenic Growth Factor Release by Dental Pulp Stem/Stromal Cells. *Materials*, 2021, 14 (9), pp.2237. 10.3390/ma14092237. hal-03547486

HAL Id: hal-03547486

<https://hal.science/hal-03547486>

Submitted on 28 Jan 2022

HAL is a multi-disciplinary open access archive for the deposit and dissemination of scientific research documents, whether they are published or not. The documents may come from teaching and research institutions in France or abroad, or from public or private research centers.

L'archive ouverte pluridisciplinaire **HAL**, est destinée au dépôt et à la diffusion de documents scientifiques de niveau recherche, publiés ou non, émanant des établissements d'enseignement et de recherche français ou étrangers, des laboratoires publics ou privés.

Article

Ultrashort Peptide Hydrogels Display Antimicrobial Activity and Enhance Angiogenic Growth Factor Release by Dental Pulp Stem/Stromal Cells

Marina E. Afami¹, Ikhlas El Karim¹ , Imad About², Sophie M. Coulter³, Garry Laverty³  and Fionnuala T. Lundy^{1,*} 

¹ Wellcome-Wolfson Institute for Experimental Medicine, School of Medicine, Dentistry and Biomedical Sciences, Queen's University Belfast, 97 Lisburn Road, Belfast BT9 7BL, UK; mafami01@qub.ac.uk (M.E.A.); i.elkarim@qub.ac.uk (I.E.K.)

² Aix Marseille Univ, CNRS, ISM, Inst Movement Sci, 13385 Marseille, France; imad.about@univ-amu.fr

³ School of Pharmacy, Queen's University Belfast, 97 Lisburn Road, Belfast BT9 7BL, UK; Sophie.Coulter@qub.ac.uk (S.M.C.); garry.laverty@qub.ac.uk (G.L.)

* Correspondence: f.lundy@qub.ac.uk

Abstract: Recent studies on peptide hydrogels have shown that ultrashort peptides (<8 amino acids) can self-assemble into hydrogels. Ultrashort peptides can be designed to incorporate antimicrobial motifs, such as positively charged lysine residues, so that the peptides have inherent antimicrobial characteristics. Antimicrobial hydrogels represent a step change in tissue engineering and merit further investigation, particularly in applications where microbial infection could compromise healing. Herein, we studied the biocompatibility of dental pulp stem/stromal cells (DPSCs) with an ultrashort peptide hydrogel, (naphthalene-2-ly)-acetyl-diphenylalanine-dilysine-OH (NapFFεKεK-OH), where the epsilon (ε) amino group forms part of the peptide bond rather than the standard amino grouping. We tested the antimicrobial properties of NapFFεKεK-OH in both solution and hydrogel form against *Staphylococcus aureus*, *Enterococcus faecalis* and *Fusobacterium nucleatum* and investigated the DPSC secretome in hydrogel culture. Our results showed NapFFεKεK-OH hydrogels were biocompatible with DPSCs. Peptides in solution form were efficacious against biofilms of *S. aureus* and *E. faecalis*, whereas hydrogels demonstrated antimicrobial activity against *E. faecalis* and *F. nucleatum*. Using an angiogenic array we showed that DPSCs encapsulated within NapFFεKεK-OH hydrogels produced an angiogenic secretome. These results suggest that NapFFεKεK-OH hydrogels have potential to serve as novel hydrogels in tissue engineering for cell-based pulp regeneration.

Keywords: antibacterial; biocompatibility; dental pulp; oral pathogen; secretome



1. Introduction

Recent progress in tissue engineering research has transformed hydrogels from their use as controlled delivery vehicles or inert cell carriers, to functional, biocompatible constructs, designed to influence the extracellular milieu in favour of tissue regeneration [1,2]. Extracellular matrix (ECM) components have been used very successfully for the development of hydrogels for tissue engineering purposes [3,4]. Indeed, new developments such as aerogels, based on natural alginate polymers are also in development for medical applications [5]. An important advantage of natural polymers, such as collagen, is its favourable biocompatibility [6]. However, variations in collagen preparation protocols (animal source and extraction methods) can lead to batch-to-batch variation in purity and yield [7], resulting in a level of unpredictability in the biochemical and/or mechanical properties of the resulting collagen hydrogel.

Self-assembling peptide hydrogels [8], represent an advanced class of hybrid (also known as smart/designer) hydrogels that are synthesised by standard peptide synthesis



methods but yet retain the advantages of naturally derived polymers. The design and synthesis of bioinspired custom peptide sequences that self-assemble into hydrogels offers the possibility of tailoring the sequence of amino acids within the peptide, so that the hydrogel's functional properties can be modified towards specific clinical applications [9]. The constituent peptides have been reported to self-assemble into nano fibrous networks to form hydrogels on the basis of the amphipathicity and/or self-complementarity of their peptide sequences [10]. Self-assembly is also facilitated by hydrophobic stacking interactions, generally in the form of π - π interactions, in the presence of aromatic amino acids (e.g., phenylalanine) or bulky groups such as 9-fluorenylmethoxycarbonyl (Fmoc) [11,12]. In general, relatively short peptide sequences (8–25 amino acids), have been employed for hydrogel synthesis [13] and in addition to retaining many of the favourable characteristics of naturally-derived proteins, they are relatively inexpensive to synthesise. Ultrashort peptides (<8 amino acids) have also been shown to self-assemble into hydrogels [14], and have the added advantage of even lower cost synthesis with increased translational potential.

Interestingly, within the class of self-assembling ultrashort peptides, it has been possible to design antimicrobial motifs, particularly those incorporating positively charged lysine residues, such that the peptides have inherent antimicrobial characteristics [15,16]. The design and synthesis of biocompatible hydrogels with antimicrobial activity is of great interest for tissue engineering purposes involving replacement of tissue in infected root canals [17–19]. It is well recognised that successful cell-based regenerative endodontics, involving transplanted cells, requires a high level of disinfection [20]. Indeed, it has been shown experimentally that residual bacteria have a critical negative effect on the success of regenerative endodontic procedures [21]. Disinfection of the root canals generally involves the use of irrigants, such as sodium hypochlorite and intracanal medicaments such as antibiotics. However, these approaches are not without their limitations and concerns have been raised that sodium hypochlorite may interfere with the ability of the regenerating pulp tissue to reattach to the dentin surface [22] and there is an urgent need to reduce antibiotic usage [23].

The dental pulp contains multipotent mesenchymal progenitor cells, known as dental pulp stem/stromal cells (DPSCs), which participate in dentin and pulp regeneration [24] and have been used in tissue engineering. To date, antimicrobial hydrogels have not been studied extensively for their biocompatibility with DPSCs or for their ability to inhibit micro-organisms (particularly those in biofilm form) relevant to tissue engineering sites such as root canals. Herein we assessed the biocompatibility of DPSCs with an ultrashort self-assembling peptide, (naphthalene-2-yl)-acetyl-diphenylalanine-dilysine-OH (NapFFεKεK-OH) whereby the epsilon (ϵ) amino group forms part of the peptide bond rather than the standard amino grouping [16]. We investigated the antimicrobial activity of NapFFεKεK-OH against *Staphylococcus aureus*, *Enterococcus faecalis* and *Fusobacterium nucleatum* and determined effects on angiogenic growth factor expression by DPSCs in NapFFεKεK-OH hydrogel culture.

2. Materials and Methods

2.1. Peptide Synthesis and Gelation

NapFFεKεK-OH was synthesised on a manual nitrogen bubbler apparatus using the 9-fluorenylmethoxycarbonyl (Fmoc) solid phase peptide synthesis chemistry as previously outlined [16]. Hydrogel formulation was achieved by a pH triggered method as previously described [16,25] and outlined in further detail in Table 1. Depending on the peptide concentration required (0.5%–2%; measured as % weight/volume (w/v)), the required amount of peptide was dissolved in an appropriate volume of deionised water (dH₂O) and titrated with 1 M sodium hydroxide (NaOH) to pH 8.5 and 0.5 M hydrochloric acid (HCl) to pH 7. Assembled hydrogels were examined by gel inversion assay to determine if they were self-supporting [16]. Hydrogels were employed in modified 3-(4,5-dimethylthiazol-2-yl)-2,5-diphenyltetrazolium bromide (MTT) assays, encapsulation studies, live/dead assays, secretome studies and bacterial susceptibility assays. The antibiofilm activities

of NapFFεKεK-OH peptides in solution were also investigated. For antibiofilm studies, NapFFεKεK-OH peptides were retained in solution by dissolving in alpha minimum essential medium (α -MEM) containing 0.005% *v/v* dimethyl sulphoxide (DMSO), as an alternative to pH triggered hydrogel formation.

Table 1. Stepwise formulation of a self-assembling pH-triggered 2% *w/v* NapFFεKεK peptide hydrogel.

| Formulation Step | Constituent | Quantity |
|------------------|----------------------------|--|
| 1 | NapFFεKεK-OH Peptide | 10 mg Preweighed |
| 2 | Deionized H ₂ O | 200 μ L (in 50 μ L aliquots) |
| 3 | 1 M NaOH | 50 μ L (in 10 μ L aliquots) |
| 4 | Deionized H ₂ O | 150 μ L (in 50 μ L aliquots) |
| 5 | 0.5 M HCl | 30 μ L (in 10 μ L aliquots) |
| 6 | Deionized H ₂ O | 50 μ L |
| 7 | 0.5 M HCl | to 500 μ L (in 5 μ L aliquots) |

2.2. Dental Pulp Cell Culture

Dental pulp samples [26] were obtained in accordance with French ethics legislation and covered by the Office for Research Ethics Committees (Northern Ireland) ethical approval number 08/NIR03/15. Dental pulp tissue was cut into fragments and cultured using the explant method [27]. DPSCs were cultured in α -MEM (Thermo Fisher Scientific, Waltham, MA, USA), supplemented with 10% heat inactivated foetal bovine serum (Thermo Fisher Scientific, Waltham, MA USA), 1% *w/v* L-glutamine (L-glut) (Thermo Fisher Scientific, Waltham, MA, USA) and 1% *w/v* penicillin + streptomycin (Thermo Fisher Scientific, Waltham, MA, USA). Cells were grown to approximately 80% confluence at 37 °C with 5% CO₂. Cells between passages 2–4 were used throughout.

2.3. Modified MTT Assay for DPSCs in 3D Culture

DPSCs (1×10^6 cells/mL) were encapsulated in 0.5% to 2% *w/v* NapFFεKεK-OH hydrogels (100 μ L) and 200 μ L of α -MEM gently added on top to establish 3D culture in 96-well plates. Viability of DPSCs encapsulated within NapFFεKεK-OH hydrogels was assessed by employing an MTT protocol, previously modified for 3D cell cultures [28]. DPSCs encapsulated in 2% *w/v* hydroxypropyl methylcellulose (HPMC) hydrogels were included as 3D controls. Cell viability was assessed at 1 and 14 days after encapsulation. Briefly, 20 μ L of MTT (5 mg/mL in Hanks balanced salt solution (HBSS)) was added to each well and incubated for 1 h at 37 °C. Media (200 μ L) was then carefully removed and replaced by 200 μ L DMSO with incubation for 10 min at 37 °C. The converted dye was eluted by shaking the plate at 220 rpm for 3 h. The supernatant from each well was transferred to a new plate and the absorbance measured at 570 nm on a microplate reader (Thermo Scientific Varioskan LUX, Warrington, UK) using SkanIt RE 4.1 software.

2.4. Visualisation of Encapsulated Cells

To visualise cell encapsulation within hydrogels by confocal microscopy, DPSCs were encapsulated in 0.5–2% *w/v* NapFFεKεK-OH hydrogels at a density of 1×10^6 cells/mL, with 100 μ L of cells encapsulated in 100 μ L of hydrogel. Prior to plating the encapsulated cells in glass bottom dishes (WillCo Wells BV, Amsterdam, The Netherlands) the bottom of each dish was marked with a hydrophobic barrier pen (Fisher Scientific, Dublin, Ireland), to retain the hydrogels within a defined area. Encapsulated DPSCs were incubated for 24 h before fixing with 4% paraformaldehyde for 30 min and then washed with phosphate buffered saline (PBS) three times. A few drops of ProLongTMGold Antifade Mountant with 4',6-diamidino-2-phenylindole (DAPI; ThermoFisher Scientific, Warrington, UK) were transferred to a circular coverslip, placed on top of the hydrogel construct and cured at room temperature for 24 h. Encapsulated DPSCs were visualised with SP8 Confocal

Microscope (Leica). Z stack images were acquired and processed using LAS X software (Leica Microsystems, Wetzlar, Germany).

2.5. Live/Dead Assay

More extensive cytotoxicity studies were undertaken on 0.5% *w/v* NapFFeKεK-OH hydrogels as this was the previously reported minimum gelation concentration [16] of the hydrogel and would have favourable injectability for use in root canals. Conditioned media collected on day 14 from 0.5% *w/v* NapFFeKεK-OH hydrogels was tested for potential cytotoxic effects on DPSCs. Cells (1×10^4 cells/mL) were plated in 96-well microtitre plates and incubated for 48 h. DPSCs were then treated with 100 μL of conditioned media for 24 h. Controls were treated with 5% *v/v* Triton-X or media. Cell viability was assessed using the live/dead viability/cytotoxicity kit, for mammalian cells (ThermoFisher Scientific, Warrington, UK) as outlined in the manufacturer's instructions. Images were captured using an Evos FL Auto Imaging System (ThermoFisher Scientific, Warrington, UK).

2.6. Antibacterial Effects

To gain insight into the antibacterial action of NapFFeKεK-OH, we tested its efficacy in both solution and hydrogel form. The antibacterial effects of low concentrations of NapFFeKεK-OH peptides in solution (representing peptides in solution that may diffuse from the hydrogel surface [15,16]) were tested against bacterial biofilms in 96-well microtitre plates. *S. aureus* (ATCC 25923) and *E. faecalis* (NCTC 12697) were grown aerobically in Müeller Hinton broth, allowed to reach mid-Log phase and then diluted to 1×10^6 colony forming units (CFU)/mL in Müeller Hinton broth (Sigma-Aldrich, Dorset, UK) to obtain inoculums for the biofilm assay. Wells containing 100 μL of inoculum were incubated aerobically for 5 h to establish initial *S. aureus* and *E. faecalis* biofilms. *F. nucleatum* (NCTC 10562) was grown anaerobically in fastidious anaerobe broth (LabM Limited, Lancashire, UK), allowed to reach mid-Log phase and diluted to 5×10^6 CFU/mL in fastidious anaerobe broth to obtain an inoculum for the biofilm assay. Wells containing 100 μL of inoculum were incubated anaerobically for 48 h to establish initial *F. nucleatum* biofilms.

After initial biofilm formation, planktonic bacteria were removed by washing with PBS and the biofilms were treated with 100 μL of 0.01% or 0.1% *w/v* NapFFeKεK-OH (dissolved in appropriate broth containing 0.005% *v/v* DMSO). Following NapFFeKεK-OH treatment, biofilms were allowed to mature either aerobically for a further 24 h (*S. aureus* and *E. faecalis*) or anaerobically for a further 48 h (*F. nucleatum*). Wells containing inoculum were also treated with vehicle controls (broth containing 0.005% *v/v* DMSO). After either 24 or 48 h incubation, planktonic bacteria were removed by washing and the biofilm biomass was quantified by the crystal violet assay [29].

The ability of the 0.5% *w/v* assembled hydrogel to reduce bacterial viability was assessed using a colony count method as previously described [30]. Briefly, *S. aureus* and *E. faecalis* were grown aerobically in Müeller Hinton broth, allowed to reach mid-Log phase and diluted to 2×10^6 CFU/mL. *F. nucleatum* was grown anaerobically in fastidious anaerobe broth, allowed to reach mid-Log phase and diluted to 5×10^6 CFU/mL. Bacterial suspensions (100 μL) were added on top of 100 μL preformed 0.5% *w/v* NapFFeKεK-OH hydrogels in 96-well plates. Untreated control wells contained inoculated broth only. After 24 h incubation 20 μL samples were removed from each well, serially diluted and 10 μL from each dilution was plated out for viability counting using the Miles and Misra method [31]. Results were displayed as mean Log_{10} CFU/mL.

2.7. Angiogenic Array

Angiogenic arrays (human angiogenesis antibody array-membrane; Abcam Cambridge UK) were employed for the simultaneous detection of 43 growth factors and cytokines in DPSCs cultured in 2D and 3D. The assay procedure was performed as described in the manufacturer's instructions, using 14 day conditioned medium from DPSCs cultured in either 0.5% *w/v* NapFFeKεK-OH hydrogels or standard 2D culture. Arrays were imaged

using a Syngene G: BOX, with GeneSys software and semiquantified using ImageJ, image analysis programme, with a microarray plugin. Results were presented as a heat map generated using Microsoft Excel.

2.8. Statistical Analysis

Results were expressed as the mean of three independent experiments with three to six replicates per experiment. GraphPad Prism Software (Version 8) was used to perform statistical analysis (GraphPad Software Inc., San Diego, CA, USA). MTT assay results were analysed by one-way ANOVA followed by Dunnett's post hoc multiple comparison test. Comparisons were made with HPMC controls in the modified MTT assay. Biofilm inhibition and bacterial viability results were analysed by Mann–Whitney non parametric tests, and comparisons were made with untreated controls or vehicle control treatments respectively. The level of statistical significance was set at $p < 0.05$.

3. Results

3.1. Peptide Hydrogels and Their Biocompatibility for 3D Culture of DPSCs

Assembled NapFFeKεK-OH peptide hydrogels (0.5–2% w/v) were shown to be self-supporting as determined by gel inversion assay (Figure 1A). Following their encapsulation into hydrogels, cells were fixed and permeabilised prior to DAPI staining and visualisation by confocal microscopy. Confocal images (Figure 1B) confirmed that DPSCs were maintained in 3D within 0.5–2% w/v hydrogels, following their encapsulation. Using a modified MTT assay, we tested the suitability of NapFFeKεK-OH hydrogels (0.5–2% w/v) for 3D culture of DPSCs after 1 and 14 days encapsulation. MTT assay results were significantly higher in all NapFFeKεK-OH hydrogels relative to the control HPMC hydrogel on day 1 following encapsulation (Figure 2A), whereas no significant differences were observed after 14 days (Figure 2B).

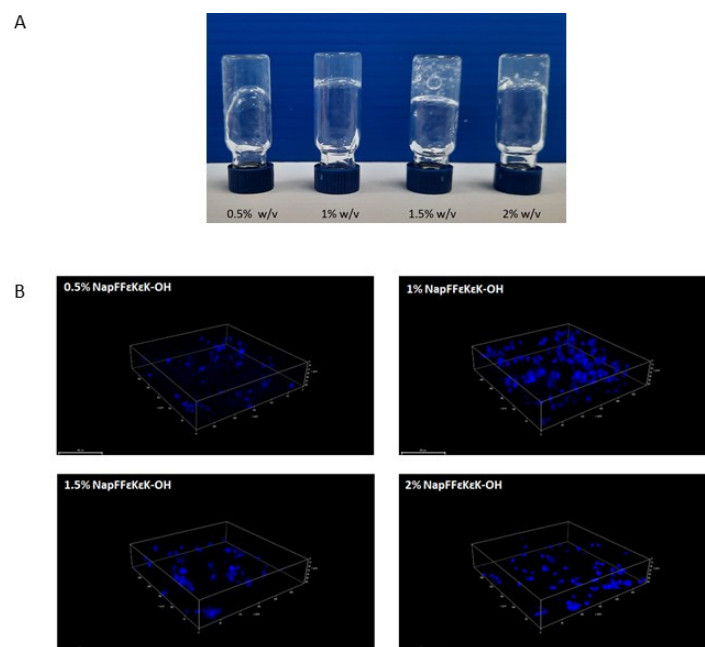


Figure 1. Formulated NapFFeKεK-OH hydrogel properties. (A) The assembled NapFFeKεK-OH hydrogels (0.5–2% w/v) were shown to be self-supporting. (B) Confocal microscopy of DPSCs 24 h after their encapsulation in 0.5–2% w/v NapFFeKεK-OH hydrogels, showed that cells were retained in 3D within the hydrogels. Cells were fixed and permeabilised within the hydrogel before staining of the encapsulated DPSC nuclei with DAPI. Images were captured using an SP8 Confocal Microscope. Scale bar: 100 μm.

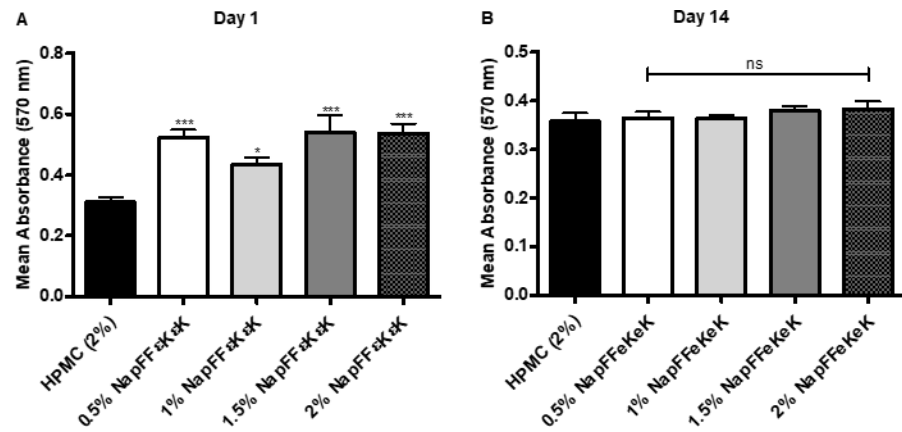


Figure 2. Modified MTT assay (for 3D culture) following encapsulation of DPSCs in NapFFeKεK-OH hydrogels (0.5%, 1%, 1.5% and 2% *w/v*) at (A) day 1 and (B) day 14. Results are the average (\pm standard error) of three independent experiments (three replicates per experiment). All comparisons were made with the HPMC control. One-way ANOVA followed by Dunnett's post hoc correction for multiple comparisons. ns: no significant difference ($p > 0.05$), *: $p \leq 0.05$, ***: $p \leq 0.001$.

3.2. Live/Dead Assay of DPSCs Incubated with 0.5% *w/v* NapFFeKεK-OH Conditioned Medium

Further studies were undertaken using conditioned media from 0.5% *w/v* NapFFeKεK-OH hydrogels, as it represented the minimum gelation concentration [16]. DPSCs treated with 0.5% *w/v* NapFFeKεK-OH conditioned media, stained green with calcein AM, indicating live cells. Very few cells stained red with EthD-1 (dead cells), suggesting little or no cytotoxicity of soluble hydrogel components present in the conditioned medium after 14 days (Figure 3).

3.3. Antibacterial Activity of NapFFeKεK-OH

It was important to determine if low concentrations (0.1%, 0.01% *w/v*) of NapFFeKεK-OH peptides (representing peptides in solution that may diffuse from the hydrogel surface) could have antimicrobial activity against biofilms of oral pathogens. Results showed that the biomass of *S. aureus* biofilms was significantly reduced when exposed to 0.1% *w/v* NapFFeKεK-OH, whereas treatment with 0.01% *w/v* peptide did not significantly alter biofilm biomass (Figure 4A,B). NapFFeKεK-OH caused a significant reduction in the biomass of *E. faecalis* biofilm at both concentrations tested (Figure 4C,D), however no reductions were observed against *F. nucleatum* biofilms (Figure 4E,F).

The antibacterial activity of the assembled 0.5% *w/v* NapFFeKεK-OH hydrogel against *S. aureus*, *E. faecalis* and *F. nucleatum* was tested using a CFU viable count assay, after 24 h bacterial growth on the hydrogel surface. There was no significant change in the number of viable colonies observed when *S. aureus* was grown on the surface of NapFFeKεK-OH (Figure 5A). However, the NapFFeKεK-OH hydrogel significantly reduced numbers of *E. faecalis* (Figure 5B) and *F. nucleatum* (Figure 5C), indicating that the hydrogel itself also had significant antimicrobial activity against these micro-organisms.

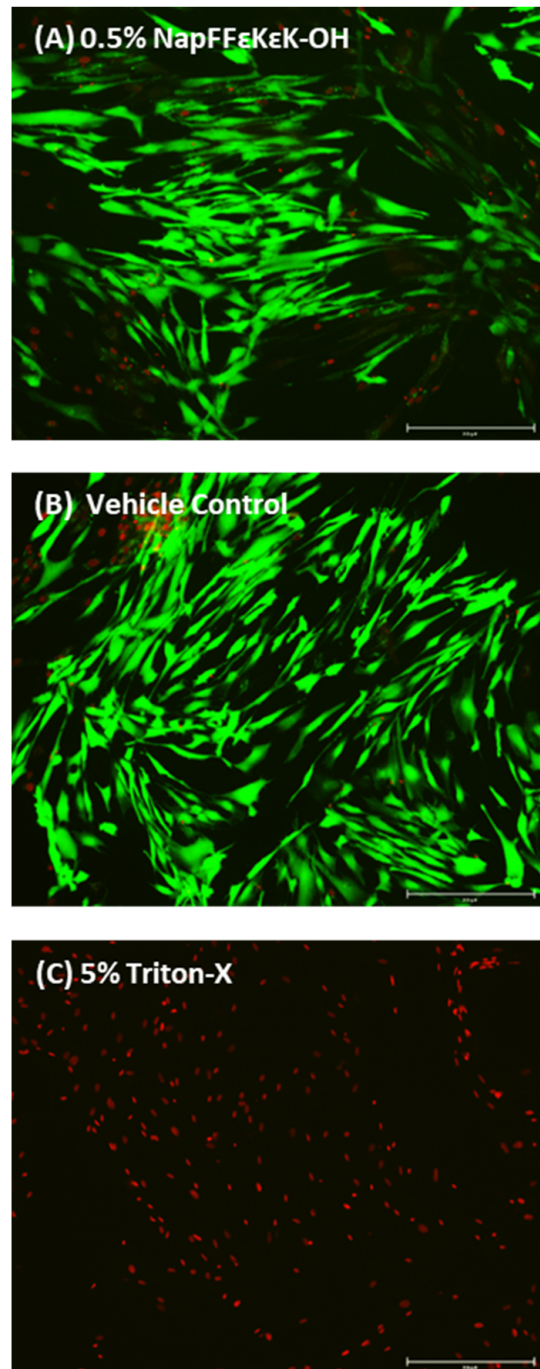


Figure 3. Live/dead viability/cytotoxicity assay showing representative images of (A) DPSCs treated with Day 14 conditioned media obtained from 0.5% *w/v* NapFFεKεK-OH hydrogels, (B) vehicle control (α -MEM incubated for 14 days at 37 °C prior to cell treatment) and (C) DPSCs treated with 5% *v/v* Triton-X. Images A and B show mainly live cells, stained green with calcein AM, with very few cells stained red, whereas in C dead cells are stained red with EthD-1. Images were captured using an Evos FL Auto Imaging System. Scale bars: 250 μ m.

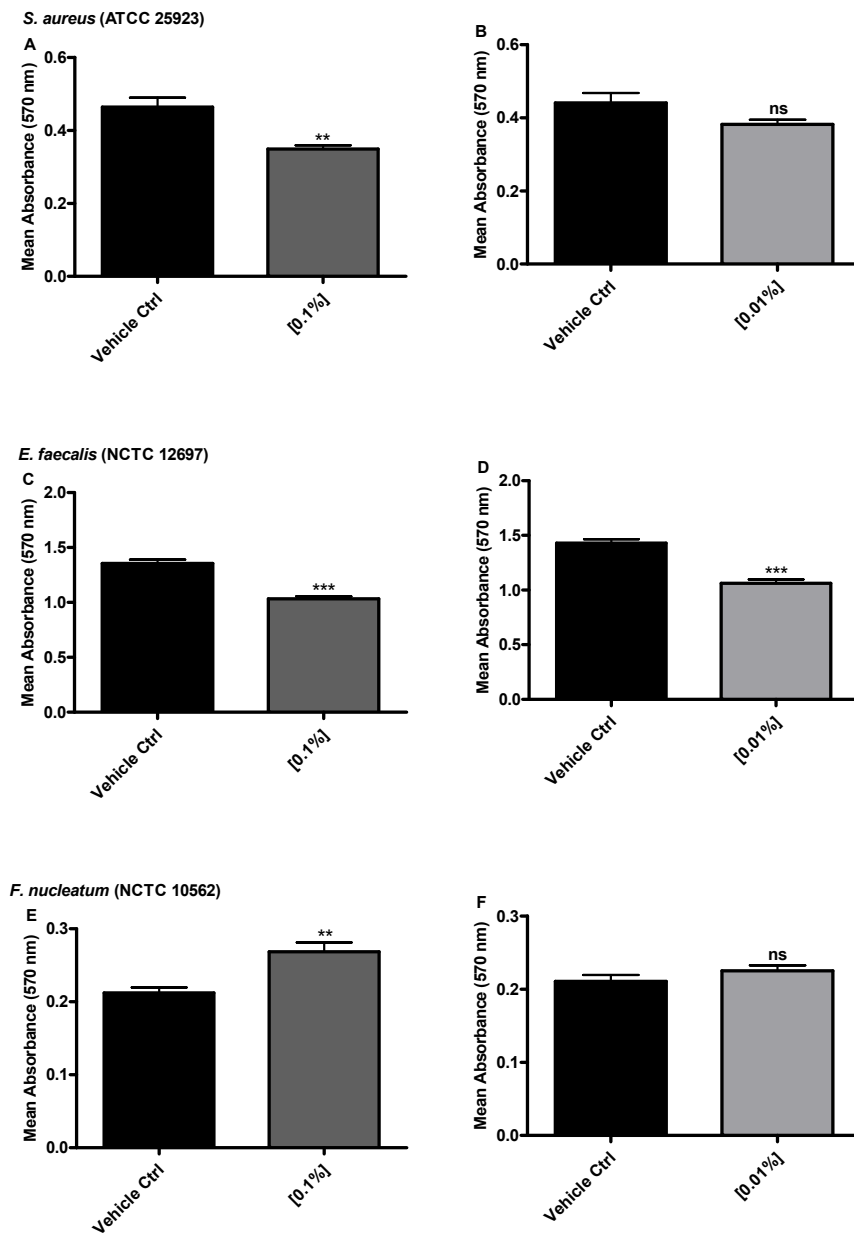


Figure 4. Biofilm inhibition determined by biofilm biomass using the crystal violet assay. (A,B) *S. aureus*, (C,D) *E. faecalis* and (E,F) *F. nucleatum* biofilm biomass after 24 h incubation with 0.1% and 0.01% *w/v* peptide concentration of NapFFεKεK-OH. Results are displayed as the average (\pm standard error) of three independent experiments (three replicates per experiment). All comparisons were made with the appropriate vehicle control. Mann-Whitney non parametric testing was employed for statistical analysis. ns: no significant difference ($p > 0.05$), **: $p \leq 0.01$, ***: $p \leq 0.001$.

3.4. Effect of Hydrogel Culture on the Angiogenic Secretome of DPSCs

An angiogenic array for the detection of 43 growth factors/cytokines was employed to test conditioned media collected from DPSCs following 14 days culture in 0.5% *w/v* NapFFεKεK-OH hydrogels compared with cells grown in standard 2D DPSC culture. Heat map comparison of DPSCs grown in 0.5% *w/v* NapFFεKεK-OH 3D hydrogel compared with 2D culture, showed upregulation of angiogenin (ANG), epidermal growth factor (EGF), epithelial neutrophil-activating peptide 78 (ENA-78), basic fibroblast growth factor (bFGF), leptin, platelet-derived growth factor-BB (PDGR-BB), vascular endothelial growth factor (VEGF) and VEGF-D, along with downregulation of interferon gamma (IFN- γ), insulin-like growth factor 1 (IGF-1), interleukin (IL)-6, placental growth factor (PLGF),

regulated upon activation normal T cell expressed and secreted (RANTES), tissue inhibitor of matrix metalloproteinases (TIMP)-1, TIMP-2, angiopoietin-1 (ANGPT1), angiopoietin-2 (ANGPT2), T lymphocyte-secreted protein I-309 (I-309), IL-10, IL-1 α , IL-1 β , IL-2, IL-4, interferon-inducible T cell alpha chemoattractant (I-TAC), monocyte chemoattractant protein (MCP)-3, MCP-4, MMP (matrix metalloproteinase)-1, MMP-9, tyrosine kinase with immunoglobulin-like and EGF-like domains (TIE-2) and tumour necrosis factor alpha (TNF α) (Figure 6).

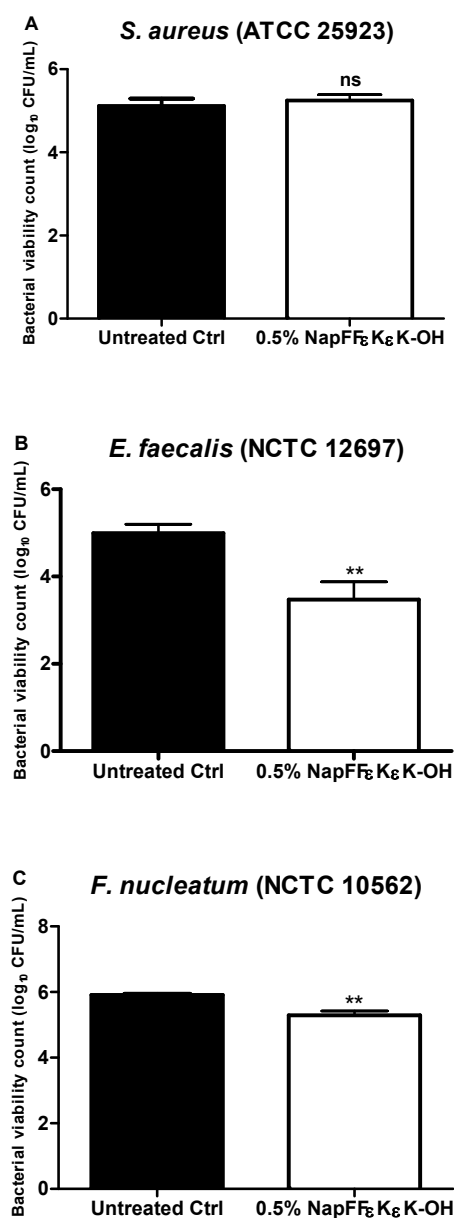


Figure 5. Bacterial viability counts (Log₁₀ CFU/mL) for (A) *S. aureus*, (B) *E. faecalis* and (C) *F. nucleatum* after 24 h growth on the surface of 0.5% *w/v* NapFF ϵ K ϵ K-OH hydrogels. Results are the average (\pm standard error) of three independent experiments (three replicates per experiment). All comparisons were made with untreated controls. Mann-Whitney non parametric testing was employed for statistical analysis. ns: no significant difference ($p > 0.05$), **: $p \leq 0.01$.

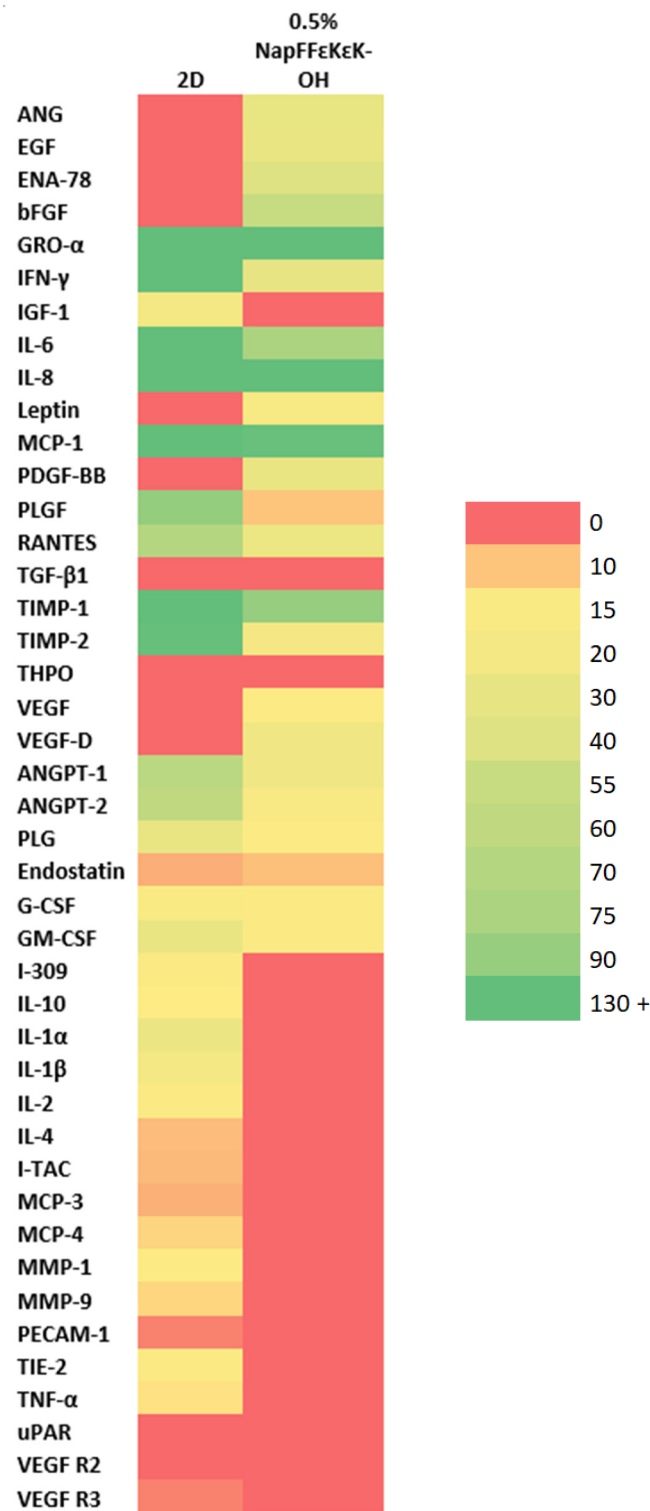


Figure 6. Heat map showing the expression of growth factors/cytokines in conditioned media from DPSCs following 14 days encapsulation in 0.5% *w/v* NapFFεKεK-OH hydrogels versus 2D culture. Heat map comparison showed upregulation of ANG, EGF, ENA-78, bFGF, leptin, PDGR-BB, VEGF and VEGF-D, along with downregulation of IFN-γ, IGF-1, IL-6, PLGF, RANTES, TIMP-1, TIMP-2, ANGPT1, ANGPT2, I-309, IL-10, IL-1α, IL-1β, IL-2, IL-4, I-TAC, MCP-3, MCP-4, MMP-1, MMP-9, TIE-2 and TNFα in 0.5% *w/v* NapFFεKεK-OH 3D hydrogel, compared with 2D culture. The heat map was generated in Excel using a 3-colour scale whereby red colour represents no expression above baseline, yellow represents the median expression level of the dataset and green represents the 90% percentile of the expression levels obtained. Colour shading and associated arbitrary values were

then generated automatically by Excel. Results represent pooled conditioned media collected from six replicates. Abbreviations: angiogenin (ANG); epidermal growth factor (EGF); epithelial neutrophil-activating peptide 78 (ENA-78); basic fibroblast growth factor (bFGF); growth-regulated alpha protein (GRO- α); interferon gamma (IFN- γ); insulin-like growth factor 1 (IGF-1); interleukin-6 (IL-6); interleukin-8 (IL-8); leptin; monocyte chemoattractant protein-1 (MCP-1); platelet-derived growth factor BB (PDGF-BB); placental growth factor (PLGF); regulated upon activation normal T cell expressed and secreted (RANTES); transforming growth factor-beta 1 (TGF- β 1); tissue inhibitor of matrix metalloproteinases-1 (TIMP-1); tissue inhibitor of matrix metalloproteinases-2 (TIMP-2); thrombopoietin (THPO); vascular endothelial growth factor (VEGF); vascular endothelial growth factor-D (VEGF-D); angiopoietin-1 (ANGPT1); angiopoietin-2 (ANGPT2); plasminogen (PLG); endostatin; granulocyte colony stimulating factor (G-CSF); granulocyte-macrophage colony-stimulating factor (GM-CSF); T lymphocyte-secreted protein I-309 (I-309); interleukin-10 (IL-10); interleukin-1 alpha (IL-1 α); interleukin-1 beta (IL-1 β); interleukin-2 (IL-2); interleukin-4 (IL-4); interferon-inducible T cell alpha chemoattractant (I-TAC); monocyte chemoattractant protein-3 (MCP-3); monocyte chemoattractant protein-4 (MCP-4); matrix metalloproteinase-1 (MMP-1); matrix metalloproteinase-9 (MMP-9); platelet and endothelial cell adhesion molecule-1 (PECAM-1); tyrosine kinase with immunoglobulin-like and EGF-like domains (TIE-2); tumour necrosis factor alpha (TNF α); urokinase plasminogen activator surface receptor (uPAR); vascular endothelial growth factor receptor 2 (VEGF R2); vascular endothelial growth factor receptor 3 (VEGF R3).

4. Discussion

In the current study, NapFF ϵ K ϵ K-OH was studied at gelation concentrations (0.5–2% *w/v*) and biocompatibility with DPSCs was demonstrated at all concentrations tested. Previous work demonstrated that NapFF ϵ K ϵ K-OH had a nanofibrous hydrogel structure, as determined by scanning electron microscopy [16]. We selected 0.5% *w/v*, for further investigation as this was the minimum gelation concentration previously reported for NapFF ϵ K ϵ K-OH to form the required hydrogel platform [16]. Such low molecular peptide hydrogelator systems form shear thinning soft gels, flowing readily upon injection and recovering their viscosity quickly after removal of shear [32]. In line with previous reports on peptides containing Fmoc-FF and Nap-FF [33,34], we proposed similar rheological properties for NapFF ϵ K ϵ K-OH. Such properties would be considered advantageous in terms of ease of handling, especially for clinical applications such as injection into root canals.

The current study builds on our previous work in which a number of ultrashort peptide hydrogels were designed and tested for their antimicrobial activities [16]. Previously we showed that NapFFKK was more antimicrobial than NapFF ϵ K ϵ K. However, we also reported that NapFFKK was particularly cytotoxic to fibroblast cell lines and that NapFF ϵ K ϵ K possessed the greatest cytocompatibility of all the peptides studied [16]. Indeed, in preliminary investigations we confirmed, as expected, that NapFFKK was toxic to DPSCs (results not shown) and it was not investigated further. Instead, we focused on investigating the biocompatibility of NapFF ϵ K ϵ K-OH against DPSCs, encapsulated within the NapFF ϵ K ϵ K-OH hydrogels, using a modified MTT assay [28]. In previous reports, biocompatibility and cell growth have been investigated on hydrogel surfaces [35,36], however, the modified MTT assay [28] has the advantage that it determines biocompatibility of cells within the hydrogel and more closely represents the cell-based therapeutic approach that would be adopted for delivery of DPSCs into root canals. Using conditioned medium obtained from 0.5% *w/v* NapFF ϵ K ϵ K-OH hydrogels, we showed that soluble components from the hydrogel did not exhibit cytotoxic effects as determined by the live/dead assay. This assay has been extensively employed for discriminating live and dead cells in various culture conditions or following cell treatments [28,36,37].

Peptide hydrogels have favourable characteristics such as chemical and functional versatility however one potential disadvantage is their cost of synthesis and purification of larger peptide/protein motifs. NapFF ϵ K ϵ K-OH has a major advantage in that it is an ultrashort peptide and therefore relatively inexpensive to synthesise and scale-up for

pharmaceutical use. Furthermore, like the majority of naturally occurring antimicrobial peptides (AMPs) [38], NapFFεKεK-OH is cationic. Cationic peptides, with excess numbers of positively charged amino acids (such as lysine, arginine and histidine), tend to exhibit antimicrobial activity as a result of their electrostatic interactions with negatively charged bacterial membranes [39]. Oral bacteria growing in biofilms have been reported to be more resistant to antimicrobial agents such as amoxicillin, metronidazole and doxycycline than planktonic cells [40,41] and additional therapeutics are therefore needed. NapFFεKεK-OH peptides in solution form (0.01% and 0.1% *w/v*) were tested for their antibiofilm properties to investigate if low concentrations of peptides in solution possess antibiofilm effects. It has previously been debated that antimicrobial activity is not exclusive to the process of gelation and that the presence of soluble peptides around the hydrogel surface could also have a role in the antimicrobial properties of the peptide [15,16]. The presence of lysine, and the cationic activity associated with it, undoubtedly contribute to the antibacterial activity observed in the current study. The peptides in solution are likely to act similarly to cationic AMPs, by targeting the bacterial membrane [39]. Furthermore, the antibiofilm activity of an AMP is not only related to its ability to interact with bacterial membrane but on its ability to penetrate the biofilm matrix [42]. NapFFεKεK-OH significantly reduced the biofilm formed by *S. aureus* only at 0.1% *w/v*, but it was able to significantly reduce biofilms formed by *E. faecalis* at both concentrations tested suggesting that NapFFεKεK-OH may exhibit different killing effects against different types of Gram positive bacteria. Moreover, no antibiofilm activity was evident against *F. nucleatum*. The structure of the bacterial cell wall differs fundamentally in Gram positive and Gram negative bacteria [43]. Whereas Gram positive bacteria have a thick peptidoglycan layer, Gram negative bacteria have a thinner peptidoglycan layer and an additional outer membrane containing lipopolysaccharide. The additional protection offered by the outer membrane [43] is thought to contribute to the tendency for Gram negative bacteria tend to be more resistant to antimicrobials (particularly in biofilm form), concurring with the results presented herein.

The use of different assays for determining antibacterial efficacy is also worth noting, as our results demonstrated both antibiofilm and bactericidal activity for NapFFεKεK-OH in solution and hydrogel form respectively. Much less is known about the potential mechanism of action of assembled peptides in the hydrogel form, but peptide self-assembly has been suggested to have a role in the antimicrobial properties of peptide hydrogels [44]. Previous work has also suggested that polymer-derived hydrogels may act via a contact-dependent involving membrane disruption [45]. Thus, presence or absence of gelation could contribute to the differences we observed in the efficacy of the hydrogel and solution forms of NapFFεKεK-OH against the same bacterial species. Moreover, the fact that a bacterial susceptibility assay was employed for determining antimicrobial activity of hydrogels whereas a biofilm assay was employed for determining the antimicrobial activity of peptides in solution, makes comparisons of peptide efficacy within the same species more challenging.

The NapFFεKεK-OH hydrogel, with its efficacy against relevant pathogenic bacteria, could contribute to restoring antimicrobial function at the initial stages of tissue regeneration in cell based regenerative endodontics. Moreover, the cells within the hydrogel are also likely to contribute antibacterial potential [46] during the dental pulp regenerative process. For example, dental pulp fibroblasts produce complement C3b for opsonisation of cariogenic bacteria [47] and also produce a membrane attack complex, which leads to pathogen lysis by osmotic shock [48].

One of the proposed benefits of growth of cells in 3D culture is that the cellular microenvironment is more physiologically relevant for tissue engineering purposes [49]. Therefore, hypothesising that hydrogel culture could offer a more favourable microenvironment for DPSCs, we assessed the angiogenic secretome of DPSCs grown in NapFFεKεK-OH compared with standard 2D culture. Angiogenesis, the sprouting of new blood vessels, plays a significant role in successful tissue engineering. So-called reparative angiogenesis, which occurs post injury or infection, recreates functional and interconnected vessels within

the tissue. It is a complex process, involving interplay between resident cells, soluble factors and extracellular matrix components. Perhaps the most important mediator of angiogenesis is vascular endothelial growth factor (VEGF), recognised to be an endothelial cell-specific mitogen and chemotactic agent that plays a significant role in the physiology of the normal vasculature. Tissue engineered scaffolds have traditionally stimulated angiogenesis by the addition of single growth factors such as VEGF [50], however sequential addition of growth factors has improved on this approach [51]. Synthesis and release of angiogenic factors by cells within the construct could provide a better alternative to mimic the complex conditions required for angiogenesis. Secretome analysis of cells encapsulated within NapFFεKεK-OH hydrogels suggested that out of five bioactive factors (VEGF, fibroblast growth factor (FGF), epidermal growth factor (EGF), platelet-derived growth factor (PDGF) and insulin-like growth factor (IGF)) commonly utilised in tissue engineering [52], all but IGF were shown to increase in NapFFεKεK-OH hydrogel versus 2D culture. Interestingly, within the dental pulp IGF is associated with osteo/odontogenic differentiation [53,54] and levels may not therefore be expected to be so closely linked with angiogenesis or vascularisation.

5. Conclusions

In conclusion, this work has identified NapFFεKεK-OH hydrogels as biocompatible with cells of the dental pulp. Given that regenerative endodontics requires tissue regeneration following infection, and that bacterial elimination from infected canals is never complete, NapFFεKεK-OH showed biocompatibility with DPSCs and antibacterial activity against oral pathogens associated with endodontic infections, and therefore holds promise for translational use. Furthermore, the encapsulated cells within these antimicrobial hydrogels, produced angiogenic factors that could contribute to pulp revascularisation *in vivo*.

Author Contributions: Conceptualization, I.E.K., I.A., G.L. and F.T.L.; Formal analysis, M.E.A.; Funding acquisition, I.E.K., G.L. and F.T.L.; Investigation, M.E.A. and S.M.C.; Methodology, S.M.C. and G.L.; Project administration, I.E.K. and F.T.L.; Resources, I.E.K., I.A., G.L. and F.T.L.; Supervision, I.E.K., G.L. and F.T.L.; Validation, M.E.A.; Visualization, M.E.A. and F.T.L.; Writing—original draft, M.E.A. and F.T.L.; Writing—review & editing, M.E.A., I.E.K., I.A., S.M.C., G.L. and F.T.L. All authors have read and agreed to the published version of the manuscript.

Funding: This work was supported by a Ph.D. Studentship from the Department for the Economy (Northern Ireland) and by the A. G. Leventis Foundation.

Institutional Review Board Statement: The study was conducted according to the guidelines of the Declaration of Helsinki, and approved by the Office for Research Ethics Committees (Northern Ireland) (08/NIR03/15, dated 11/04/08).

Informed Consent Statement: Informed consent was obtained from all subjects involved in the study.

Data Availability Statement: The data presented in this study are available on request from the corresponding author.

Acknowledgments: The authors gratefully acknowledge the skilful technical assistance of Catherine Fulton.

Conflicts of Interest: The authors declare no conflict of interest.

References

1. Boso, D.; Maghin, E.; Carraro, E.; Giagante, M.; Pavan, P.; Piccoli, M. Extracellular Matrix-Derived Hydrogels as Biomaterial for Different Skeletal Muscle Tissue Replacements. *Materials* **2020**, *13*, 2483. [[CrossRef](#)]
2. Li, K.; Zhu, Y.; Zhang, Q.; Shi, X.; Liang, F.; Han, D. A self-healing hierarchical fiber hydrogel that mimics ECM structure. *Materials* **2020**, *13*, 5277. [[CrossRef](#)]
3. Gomez-Florit, M.; Pardo, A.; Domingues, R.M.A.; Graça, A.L.; Babo, P.S.; Reis, R.L.; Gomes, M.E. Natural-Based Hydrogels for Tissue Engineering Applications. *Molecules* **2020**, *25*, 5858. [[CrossRef](#)] [[PubMed](#)]

4. Catoira, M.C.; Fusaro, L.; Francesco, D.D.; Ramella, M.; Boccafoschi, F. Overview of natural hydrogels for regenerative medicine applications. *J. Mater. Sci. Mater. Med.* **2019**, *30*, 115. [[CrossRef](#)] [[PubMed](#)]
5. Baldino, L.; Cardea, S.; Scognamiglio, M.; Reverchon, E. A new tool to produce alginate-based aerogels for medical applications, by supercritical gel drying. *J. Supercrit. Fluids* **2019**, *146*, 152–158. [[CrossRef](#)]
6. Antoine, E.E.; Vlachos, P.P.; Rylander, M.N. Review of Collagen I Hydrogels for Bioengineered Tissue Microenvironments: Characterization of Mechanics, Structure, and Transport. *Tissue Eng. Part B Rev.* **2014**, *20*, 683–696. [[CrossRef](#)]
7. Abraham, L.C.; Zuena, E.; Perez-Ramirez, B.; Kaplan, D.L. Guide to collagen characterization for biomaterial studies. *J. Biomed. Mater. Res. Part B Appl. Biomater.* **2008**, *87B*, 264–285. [[CrossRef](#)] [[PubMed](#)]
8. Zamuner, A.; Cavo, M.; Scaglione, S.; Messina, G.; Russo, T.; Gloria, A.; Marletta, G.; Dettin, M. Design of Decorated Self-Assembling Peptide Hydrogels as Architecture for Mesenchymal Stem Cells. *Materials* **2016**, *9*, 727. [[CrossRef](#)] [[PubMed](#)]
9. McCloskey, A.; Gilmore, B.; Lavery, G. Evolution of Antimicrobial Peptides to Self-Assembled Peptides for Biomaterial Applications. *Pathogens* **2014**, *3*, 791–821. [[CrossRef](#)]
10. Yadav, N.; Chauhan, M.K.; Chauhan, V.S. Short to ultrashort peptide-based hydrogels as a platform for biomedical applications. *Biomater. Sci.* **2020**, *8*, 84–100. [[CrossRef](#)] [[PubMed](#)]
11. Mahler, A.; Reches, M.; Rechter, M.; Cohen, S.; Gazit, E. Rigid, Self-Assembled Hydrogel Composed of a Modified Aromatic Dipeptide. *Adv. Mater.* **2006**, *18*, 1365–1370. [[CrossRef](#)]
12. Tang, C.; Ulijn, R.V.; Saiani, A. Effect of Glycine Substitution on Fmoc-Diphenylalanine Self-Assembly and Gelation Properties. *Langmuir* **2011**, *27*, 14438–14449. [[CrossRef](#)]
13. Holmes, T.C.; de Lacalle, S.; Su, X.; Liu, G.; Rich, A.; Zhang, S. Extensive neurite outgrowth and active synapse formation on self-assembling peptide scaffolds. *Proc. Natl. Acad. Sci. USA* **2000**, *97*, 6728–6733. [[CrossRef](#)]
14. Hauser, C.A.E.; Deng, R.; Mishra, A.; Loo, Y.; Khoe, U.; Zhuang, F.; Cheong, D.W.; Accardo, A.; Sullivan, M.B.; Riekkel, C.; et al. Natural tri- to hexapeptides self-assemble in water to amyloid β -type fiber aggregates by unexpected α -helical intermediate structures. *Proc. Natl. Acad. Sci. USA* **2011**, *97*, 1361–1366. [[CrossRef](#)]
15. Salick, D.A.; Kretsinger, J.K.; Pochan, D.J.; Schneider, J.P. Inherent Antibacterial Activity of a Peptide-Based β -Hairpin Hydrogel. *J. Am. Chem. Soc.* **2007**, *129*, 14793–14799. [[CrossRef](#)] [[PubMed](#)]
16. Lavery, G.; McCloskey, A.P.; Gilmore, B.F.; Jones, D.S.; Zhou, J.; Xu, B. Ultrashort Cationic Naphthalene-Derived Self-Assembled Peptides as Antimicrobial Nanomaterials. *Biomacromolecules* **2014**, *15*, 3429–3439. [[CrossRef](#)]
17. Galler, K.M.; Hartgerink, J.D.; Cavender, A.C.; Schmalz, G.; D'Souza, R.N. A Customized Self-Assembling Peptide Hydrogel for Dental Pulp Tissue Engineering. *Tissue Eng. Part A* **2012**, *18*, 176–184. [[CrossRef](#)]
18. Steindorff, M.M.; Lehl, H.; Winkel, A.; Stiesch, M. Innovative approaches to regenerate teeth by tissue engineering. *Arch. Oral Biol.* **2014**, *59*, 158–166. [[CrossRef](#)] [[PubMed](#)]
19. Wang, H.; Wang, S.; Cheng, L.; Jiang, Y.; Melo, M.A.S.; Weir, M.D.; Oates, T.W.; Zhou, X.; Xu, H.H. Novel dental composite with capability to suppress cariogenic species and promote non-cariogenic species in oral biofilms. *Mater. Sci. Eng. C* **2019**, *94*, 587–596. [[CrossRef](#)] [[PubMed](#)]
20. Fouad, A.F. The microbial challenge to pulp regeneration. *Adv. Dent. Res.* **2011**, *23*, 285–289. [[CrossRef](#)] [[PubMed](#)]
21. Verma, P.; Nosrat, A.; Kim, J.R.; Price, J.B.; Wang, P.; Bair, E.; Xu, H.H.; Fouad, A.F. Effect of Residual Bacteria on the Outcome of Pulp Regeneration In Vivo. *J. Dent. Res.* **2017**, *96*, 100–106. [[CrossRef](#)]
22. Ring, K.C.; Murray, P.E.; Namerow, K.N.; Kuttler, S.; Garcia-Godoy, F. The Comparison of the Effect of Endodontic Irrigation on Cell Adherence to Root Canal Dentin. *J. Endod.* **2008**, *34*, 1474–1479. [[CrossRef](#)] [[PubMed](#)]
23. National Institute for Health and Care Excellence (NICE); Public Health England (PHE). *Summary of Antimicrobial Prescribing Guidance—Managing Common Infections*; NICE and PHE: London, UK, 2021. Available online: <https://www.nice.org.uk/Media/Default/About/what-we-do/NICE-guidance/antimicrobial%20guidance/summary-antimicrobial-prescribing-guidance.pdf> (accessed on 22 March 2021).
24. Gronthos, S.; Mankani, M.; Brahimi, J.; Robey, P.G.; Shi, S. Postnatal human dental pulp stem cells (DPSCs) in vitro and in vivo. *Proc. Natl. Acad. Sci. USA* **2000**, *97*, 13625–13630. [[CrossRef](#)]
25. Albadr, A.A.; Coulter, S.M.; Porter, S.L.; Thakur, R.R.S.; Lavery, G. Ultrashort self-assembling peptide hydrogel for the treatment of fungal infections. *Gels* **2018**, *4*, 48. [[CrossRef](#)] [[PubMed](#)]
26. About, I.; Bottero, M.J.; de Denato, P.; Camps, J.; Franquin, J.C.; Mitsiadis, T.A. Human Dentin Production in Vitro. *Exp. Cell Res.* **2000**, *258*, 33–41. [[CrossRef](#)] [[PubMed](#)]
27. Hilken, P.; Gervois, P.; Fanton, Y.; Vanormelingen, J.; Martens, W.; Struys, T.; Politis, C.; Lambrichts, I.; Bronckaers, A. Effect of isolation methodology on stem cell properties and multilineage differentiation potential of human dental pulp stem cells. *Cell Tissue Res.* **2013**, *353*, 65–78. [[CrossRef](#)]
28. Galler, K.M.; Brandl, F.P.; Kirchhof, S.; Widbiller, M.; Eidt, A.; Buchalla, W.; Göpferich, A.; Schmalz, G. Suitability of Different Natural and Synthetic Biomaterials for Dental Pulp Tissue Engineering. *Tissue Eng. Part A* **2018**, *24*, 234–244. [[CrossRef](#)]
29. Stepanovic, S.; Vukovic, D.; Dakic, I.; Savic, B.; Švabic Vlahovic, M. A modified microtiter-plate test for quantification of staphylococcal biofilm formation. *J. Microbiol. Methods* **2000**, *40*, 175–179. [[CrossRef](#)]
30. McCloskey, A.P.; Gilmore, S.M.; Zhou, J.; Draper, E.R.; Porter, S.; Gilmore, B.F.; Xu, B.; Lavery, G. Self-assembling ultrashort NSAID-peptide nanosponges: Multifunctional antimicrobial and anti-inflammatory materials. *RSC Adv.* **2016**, *6*, 114738–114749. [[CrossRef](#)]

31. Miles, A.A.; Misra, S.S.; Irwin, J.O. The estimation of the bactericidal power of the blood. *Epidemiol. Infect.* **1938**, *38*, 732–749. [[CrossRef](#)]
32. Das, A.K.; Gavel, P.K. Low molecular weight self-assembling peptide-based materials for cell culture, antimicrobial, anti-inflammatory, wound healing, anticancer, drug delivery, bioimaging and 3D bioprinting applications. *Soft Matter* **2020**, *16*, 10065–10095. [[CrossRef](#)]
33. Yan, C.; Altunbas, A.; Yucel, T.; Nagarkar, R.P.; Schneider, J.P.; Pochan, D.J. Injectable solid hydrogel: Mechanism of shear-thinning and immediate recovery of injectable β -hairpin peptide hydrogels. *Soft Matter* **2010**, *6*, 5143–5156. [[CrossRef](#)] [[PubMed](#)]
34. Draper, E.R.; Adams, D.J. Low-Molecular-Weight Gels: The State of the Art. *Chem* **2017**, *3*, 390–410. [[CrossRef](#)]
35. Almeida, L.D.F.; Babo, P.S.; Silva, C.R.; Rodrigues, M.T.; Hebling, J.; Reis, R.L.; Gomes, M.E. Hyaluronic acid hydrogels incorporating platelet lysate enhance human pulp cell proliferation and differentiation. *J. Mater. Sci. Mater. Med.* **2018**, *29*, 88. [[CrossRef](#)]
36. Sedláček, T.; Acar, O.K.; Studenová, H.; Kotelnikov, I.; Kucáka, J.; Konečná, Z.; Zikmund, T.; Kaiser, J.; Kose, G.T.; Rypáček, F. Chondrogenic potential of macroporous biodegradable cryogels based on synthetic poly(α -amino acids). *Soft Matter* **2018**, *14*, 228–238. [[CrossRef](#)]
37. Moshaverinia, A.; Chen, C.; Akiyama, K.; Ansari, S.; Xu, X.; Chee, W.W.; Schricker, S.R.; Shi, S. Alginate hydrogel as a promising scaffold for dental-derived stem cells: An in vitro study. *J. Mater. Sci. Mater. Med.* **2012**, *23*, 3041–3051. [[CrossRef](#)]
38. Marshall, S.H.; Arenas, G. Antimicrobial peptides: A natural alternative to chemical antibiotics and a potential for applied biotechnology. *Electron. J. Biotechnol.* **2003**, *6*. [[CrossRef](#)]
39. Brogden, K.A. Antimicrobial peptides: Pore formers or metabolic inhibitors in bacteria? *Nat. Rev. Microbiol.* **2005**, *3*, 238–250. [[CrossRef](#)]
40. Shani, S.; Friedman, M.; Steinberg, D. The Anticariogenic Effect of Amine Fluorides on *Streptococcus sobrinus* and Glucosyltransferase in Biofilms. *Caries Res.* **2000**, *34*, 260–267. [[CrossRef](#)]
41. Larsen, T. Susceptibility of *Porphyromonas gingivalis* in biofilms to amoxicillin, doxycycline and metronidazole. *Oral Microbiol. Immunol.* **2002**, *17*, 267–271. [[CrossRef](#)]
42. Mai, S.; Mauger, M.T.; Niu, L.-N.; Barnes, J.B.; Kao, S.; Bergeron, B.E.; Ling, J.-Q.; Tay, F.R. Potential applications of antimicrobial peptides and their mimics in combating caries and pulpal infections. *Acta Biomater.* **2017**, *49*, 16–35. [[CrossRef](#)]
43. Epand, R.M.; Walker, C.; Epand, R.F.; Magarvey, N.A. Molecular mechanisms of membrane targeting antibiotics. *Biochim. Biophys. Acta (BBA) Biomembr.* **2016**, *1858*, 980–987. [[CrossRef](#)] [[PubMed](#)]
44. Tian, X.; Sun, F.; Zhou, X.R.; Luo, S.Z.; Chen, L. Role of peptide self-assembly in antimicrobial peptides. *J. Pept. Sci.* **2015**, *21*, 530–539. [[CrossRef](#)] [[PubMed](#)]
45. Veiga, A.S.; Schneider, J.P. Antimicrobial hydrogels for the treatment of infection. *Biopolymers* **2013**, *100*, 637–644. [[CrossRef](#)]
46. Lundy, F.T.; Irwin, C.R.; McLean, D.F.; Linden, G.J.; Karim, I.A.E. Natural Antimicrobials in the Dental Pulp. *J. Endod.* **2020**, *46*, S2–S9. [[CrossRef](#)] [[PubMed](#)]
47. Fournis, L.; Hadjichristou, C.; Jeanneau, C.; About, C.; I. Human pulp fibroblast implication in phagocytosis via complement activation. *J. Endod.* **2015**, *45*, 584–590. [[CrossRef](#)]
48. Jeanneau, C.; Rufas, P.; Rombouts, C.; Giraud, T.; Dejoui, J.; About, I. Can Pulp Fibroblasts Kill Cariogenic Bacteria? Role of Complement Activation. *J. Dent. Res.* **2015**, *94*, 1765–1772. [[CrossRef](#)]
49. Lutolf, M.P.; Hubbell, J.A. Synthetic biomaterials as instructive extracellular microenvironments for morphogenesis in tissue engineering. *Nat. Biotechnol.* **2005**, *23*, 47–55. [[CrossRef](#)]
50. Yamaguchi, N.; Zhang, L.; Chae, B.S.; Palla, C.S.; Furst, E.M.; Kiick, K.L. Growth Factor Mediated Assembly of Cell Receptor-Responsive Hydrogels. *J. Am. Chem. Soc.* **2007**, *129*, 3040–3041. [[CrossRef](#)]
51. Tengood, J.E.; Ridenour, R.; Brodsky, R.; Russell, A.J.; Little, S.R. Sequential Delivery of Basic Fibroblast Growth Factor and Platelet-Derived Growth Factor for Angiogenesis. *Tissue Eng. Part A* **2011**, *17*, 1181–1189. [[CrossRef](#)] [[PubMed](#)]
52. Mastrullo, V.; Cathery, W.; Velliou, E.; Madeddu, P.; Campagnolo, P. Angiogenesis in Tissue Engineering: As Nature Intended? *Front. Bioeng. Biotechnol.* **2020**, *8*, 188. [[CrossRef](#)] [[PubMed](#)]
53. Lv, T.; Wu, Y.; Mu, C.; Liu, G.; Yan, M.; Xu, X.; Wu, H.; Du, J.; Yu, J.; Mu, J. Insulin-like growth factor 1 promotes the proliferation and committed differentiation of human dental pulp stem cells through MAPK pathways. *Arch. Oral Biol.* **2016**, *72*, 116–123. [[CrossRef](#)] [[PubMed](#)]
54. Alkharobi, H.E.; Al-Khafaji, H.; Beattie, J.; Devine, D.A.; El-Gendy, R. Insulin-Like Growth Factor Axis Expression in Dental Pulp Cells Derived from Carious Teeth. *Front. Bioeng. Biotechnol.* **2018**, *6*, 36. [[CrossRef](#)] [[PubMed](#)]